

Prediction of Ultimate Load at the CFRP-Concrete Interface under Pure Shear Mode

Mohsen A. Issa^{1,*}, Momenur Rahman², Rajai Alrousan³

¹Department of Civil and Materials Engineering, University of Illinois at Chicago, Chicago, USA

²University of Illinois at Chicago, Chicago, USA

³Department of Civil Engineering, Jordan University of Science and Technology, Irbid, Jordan

Abstract The bond strength characteristics between Carbon Fiber Reinforced Polymer (CFRP) and concrete were investigated by conducting double face shear type pullout test. A simplified experimental setup was designed for the test to eliminate the eccentricity of active load across the bond interface. The objective of the study is to determine the ultimate bond strength and corresponding slip of CFRP-concrete interface using maximum bond stress (τ_{max}). The effect of the concrete compressive strength (f'_c) and CFRP bond width (b_f) were considered as key parameters. The results indicated that the ultimate load (P_u) increased with the increase in f'_c and b_f . On the other hand, the slip (s_o) at τ_{max} increased as a result of increasing concrete f'_c and decreased with increasing b_f . Moreover, the failure mode was more brittle with higher concrete f'_c and/or smaller CFRP b_f . An analytical model is proposed to predict the ultimate pullout load (P_u) and slip (s_o) at ultimate load. The proposed model provided a good prediction for P_u , τ_{max} , and s_o for the bond between the CFRP and concrete.

Keywords CFRP, Concrete, Bond stress, Ultimate bond capacity, CFRP-concrete interface

1. Introduction

Externally bonded Fiber Reinforced Polymer (FRP) plates or sheets have been widely used to retrofit and rehabilitate deteriorated concrete structures. These materials provide several advantages attributed to their light weight, high strength characteristics, and ease of installation. The design of FRP plates or sheets is controlled by the bond characteristics between the FRP and concrete substrate [1, 2]. Plenty of research was carried out in the past decade to evaluate the bond stress-slip behavior at the FRP-concrete interface both experimentally and analytically. Several prediction models were developed; however, a unified simple formula is desired to estimate the pullout load or the anchorage area for strengthening or retrofitting of RC structures with CFRP.

The paper presents an experimental investigation to evaluate the ultimate bond strength between CFRP laminates and concrete. The CFRP laminates were adhered on both faces of the concrete prism using epoxy. Previous studies measured the bond stress and slip at different levels using strain gauges and/or Linear Variable Displacement Transducers (LVDTs) in order to determine the effective bond length (L_e) and the maximum bond strength (τ_{max}) at the

FRP concrete interface. The test was simplified by using a single LVDT on each side of the CFRP-concrete interface. The study took into account of different bond configurations and concrete strength. In addition, an analytical model was developed to predict the test results. The analytical model can be used to determine the bond area required to resist a given load for strengthening RC structural members with externally bonded CFRP sheet.

2. Background

Chen and Teng [3] investigated the anchorage strength properties of both FRP-to-concrete and steel plate-to-concrete bonded joints. They reviewed and assessed existing anchorage strength models using experimental data collected from literature and proposed a new design model based on existing experimental observations. Lu et al. [4] proposed three different models to predict the strength characteristics and bond slip between FRP and concrete. They collected experimental data from the literature and observed that most of the studies did not consider enough parameters to capture the bond-slip behavior. Moreover, they observed some scattering in the experimental results for several studies [5-8] in their database [4]. The scattering was detected in the trend of the ultimate load (P_u) between specimens with different configurations as well as between identical specimens. This scattering and inconsistency in the test results can affect the accuracy of the prediction model [4]. Therefore, it is essential to investigate all the factors

* Corresponding author:

missa@uic.edu (Mohsen A. Issa)

Published online at <http://journal.sapub.org/cmaterials>

Copyright © 2016 Scientific & Academic Publishing. All Rights Reserved

influencing the bond properties including the testing setup and equipment when testing the bond slip behavior between FRP and concrete.

Dai *et al.* [9] conducted a single lap pullout test using 26 specimens to capture the bond stress-slip behavior at the FRP-concrete interface using different FRP types (CFRP, Aramid FRP, Glass FRP) and three different types of adhesives. They developed a nonlinear model based on interfacial fracture energy (G_f) and interfacial ductility index. McSweeney and Lopez [10] investigated the bond-slip behavior at the CFRP-concrete interface using different CFRP bond width (b_f), thickness (t_f), bond lengths (L), and varying concrete f'_c . They observed that the CFRP b_f and t_f and the concrete f'_c significantly affected the P_u while the FRP L didn't show any notable effect. Fawzia *et al.* [11] concluded that the FRP t_f has significant effect on P_u , while L exceeding the effective bond length (L_e) didn't show any notable effect. Ko *et al.* [12] reported that concrete f'_c , FRP stiffness, and G_f are the main contributing factors for the bond stress-slip behavior. They observed that the adhesive's strength and stiffness have no significant effect on the bond-slip behavior.

Studies reported in literature considered the FRP L effect on P_u as insignificant when it exceeds L_e . Maeda *et al.* [13] reported that the P_u for CFRP strips did not increase for any L above 100 mm. Nakaba *et al.* [14] reported that the bond failure by FRP delamination occurs when L is less than 100 mm, while failure by FRP rupture takes place when the anchorage length is relatively large (greater than 300 mm). Several studies [3, 4, 13-18] proposed empirical formulas to estimate the L_e . **Table 1** summarizes the proposed L_e models obtained from the literature.

Another notable factor reported by previous studies on the bond-slip behavior at the FRP-concrete interface is the effect of acting load's eccentricity. This eccentricity can occur due to misalignment in the tested specimens and/or applied load. The eccentricity of acting force when testing the bond between FRP and concrete under a single shear/lap joint test can induce undesirable flexural stresses that can influence the failure mode of the bonded assembly [19]. Nakaba *et al.*

[14] performed experiments using laminates in both faces of the concrete prism and observed that it was not possible to avoid load eccentricity when specimens were set on the loading machine. In order to eliminate the effect of acting force's eccentricity they modified P_u by multiplying it with a correction factor.

A special experimental setup was designed for this study to eliminate the eccentricity across the concrete-bond interface. The bond slip behavior was investigated by conducting a double face shear type pullout test. The double shear type pullout test was conducted by holding the concrete blocks to the testing bed with a steel plate covering the top surface and anchored to the testing bed using threaded bolts. The steel plate was designed to cover the entire concrete surface in order to prevent failure of the concrete block at its leading edge with the CFRP.

3. Research Objective and Significance

Two parameters were considered for investigation: (1) effect of CFRP bond width (b_f), and (2) effect of concrete ultimate compressive strength (f'_c) on the bond strength behavior at the CFRP-concrete interface. This study has the following research significances:

1. The study developed a simple experimental setup that eliminates the acting load's eccentricity across the CFRP-concrete bond interface.
2. Performed a parametric study with ample number (thirty) of test specimens considering the major aforementioned key parameters, so that the characteristics of CFRP-concrete bond interface can be captured.
3. A prediction model to calculate ultimate bond strength and corresponding slip model was developed based on regression analysis of experimental test results. The proposed model is simple and capable of predicting the ultimate bond strength, and the slip in terms of maximum bond stress.

Table 1. Existing Models for Ultimate Load (P_u) and Effective Bond Length (L_e)

Source	Ultimate Bond Load Model, P_u	Effective Bond Length, L_e
Maeda <i>et al.</i> (1997)	$110.2 \times 10^{-6} E_f t_f L_e b_f$	$L_e = e^{6.13 - 0.58 \ln E_f t_f}$
Khalifa <i>et al.</i> (1998)	$110.2 \times 10^{-6} (f'_c/42)^{2/3} E_f t_f L_e b_f$	$L_e = e^{6.13 - 0.58 \ln E_f t_f}$
Chen and Teng (2001)	$0.427 \beta_w (f'_c)^{0.5} L_e b_f$	$L_e = (E_f t_f / (f'_c)^{0.5})^{0.5}$
Yang <i>et al.</i> (2001)*	$(0.5 + 0.08 (E_f t_f / 100 f'_c)^{0.5}) L_e b_f \tau_u$	$L_e = 100 \text{ mm}, \tau_u = 0.5 f_i$
Iso (2003)*	$0.93 f'_c{}^{0.44} b_f L_e$ Where $L_e = L$ if $L > L$	$L_e = 0.125 (E_f t_f)^{0.57}$
Lu <i>et al.</i> (2005)	$b_f \beta_l (2 E_f t_f G_f)^{0.5}$ if $L > L_e$, $\beta_l = 1$ if $L \leq L_e$, $\beta_l = \sin(\pi L / 2 L_e)$	$L_e = a + \frac{1}{2 \lambda_1} \ln \frac{\lambda_1 + \lambda_2 \tan(\lambda_2 a)}{\lambda_1 - \lambda_2 \tan(\lambda_2 a)}$
Wu <i>et al.</i> (2009)	$0.595 b_p f'_c{}^{0.1} (E_f t_f)^{0.54}$ if $L > L_e$ $0.595 b_p f'_c{}^{0.1} (E_f t_f)^{0.54} (L/L_e)^{1.2}$ if $L < L_e$	$L_e = 0.395 (E_f t_f)^{0.54} / f'_c{}^{0.09}$

Note: All units are in SI.

*Referred to Ahmed, E.Y. S *et al.* [18]

4. Experimental Program

Test Specimens

The mechanical properties of CFRP sheets and the epoxy bonding agent (epoxy resin) are summarized in **Table 2**. Rectangular concrete prism of $150 \times 150 \times 525$ mm ($6 \times 6 \times 21$ in.) were cast and cured in the lab and then were cut into small prisms using a diamond blade saw-cut according to the desired length required for testing. **Fig. 1** shows the bond-slip test configuration for CFRP sheets and concrete for all the specimens. The CFRP sheets were adhered to the concrete specimens after being moisture cured for 28 days. The details of the tested specimens are shown in **Table 3**.

Specimen Details

Fifteen different CFRP-concrete bond configurations were used. Each configuration consisted of two specimens, thus total of thirty (30) specimens were tested. The test configurations were divided into three groups (see **Table 3**). Each group represents different concrete f'_c . Each group consisted of ten specimens with five different CFRP b_f ranging from 25 to 75 mm (1 to 3 in.). For the specimen designation shown in **Table 3**, the first letter "C" indicates the concrete f'_c and is followed by the numbers 6.2, 7.7, and

8.8 that stand for the f'_c of 6200 psi, 7700 psi, and 8800 psi, respectively. This is followed by the letter "L" which stands for the CFRP L and is followed by a numbers 4.5 indicating the L in inches. Finally, the letter "B" stands for the CFRP b_f and is followed by the numbers 1, 1.5, 2, 2.5 and 3 indicating the b_f in inches.

Table 2. Materials Properties of CFRP and Epoxy

CFRP ⁽¹⁾	Ultimate strength	620 ksi (4275 MPa)
	Design strength	570 ksi (3930 MPa)
	Modulus of elasticity	33,500 ksi (231 GPa)
	Ultimate strain	0.017 mm/mm
	Thickness	0.0065 inch (0.165 mm)
Epoxy ⁽²⁾	Maximum stress	8 ksi (55 MPa)
	Stress at rupture	7.9 ksi (54.5 MPa)
	Maximum strain	0.03 mm/mm
	Yield strain	0.025 mm/mm
	Modulus of elasticity	440 ksi (3 GPa)

(1) Mechanical Properties were tested at UIC laboratory

(2) Mechanical properties were provided by the manufacturer

Table 3. Details of the Bond Slip Specimens

Group Number	Specimen Designation	f'_c , MPa (psi)	L , mm (in.)	b_f , mm (in.)	τ_{max} , MPa (psi)	s_0 , mm (in.)	P_u , kN (Kips)
I	C8.8L4.5B1	60.7 (8800)	113 (4.5)	25 (1)	4.05(587)	0.122 (0.0048)	7.3 (1.64)
	C8.8L4.5B1.5			38 (1.5)	4.06 (588)	0.109 (0.00428)	11 (2.46)
	C8.8L4.5B2			50 (2)	4.39 (637)	0.096 (0.00377)	15.8 (3.55)
	C8.8L4.5B2.5			63 (2.5)	4.55 (661)	0.086 (0.00338)	19.9 (4.47)
	C8.8L4.5B3			75 (3)	4.54 (658)	0.08 (0.00316)	23.7 (5.33)
II	C7.7L4.5B1	53.1 (7700)	113 (4.5)	25 (1)	3.01 (436)	0.00417 (0.106)	5.9 (1.33)
	C7.7L4.5B1.5			38 (1.5)	3.24 (469)	0.0036 (0.0912)	9.5 (2.15)
	C7.7L4.5B2			50 (2)	3.30 (479)	0.0032 (0.0822)	13 (2.92)
	C7.7L4.5B2.5			63 (2.5)	3.49 (505)	0.0029 (0.0739)	16.6 (3.73)
	C7.7L4.5B3			75 (3)	3.61 (523)	0.0026 (0.0655)	20.6 (4.64)
III	C6.2L4.5B1	42.7 (6200)	113 (4.5)	25 (1)	3.44 (499)	0.00478 (0.1214)	6.4 (1.44)
	C6.2L4.5B1.5			38 (1.5)	3.81 (552)	0.004 (0.1016)	10.6 (2.39)
	C6.2L4.5B2			50 (2)	3.89 (564)	0.00361 (0.0916)	14.5 (3.26)
	C6.2L4.5B2.5			63 (2.5)	4.09 (593)	0.00325 (0.0826)	18.5 (4.15)
	C6.2L4.5B3			75 (3)	4.15 (601)	0.0029 (0.0748)	22.4 (5.04)

Note: Two specimens were tested for each case

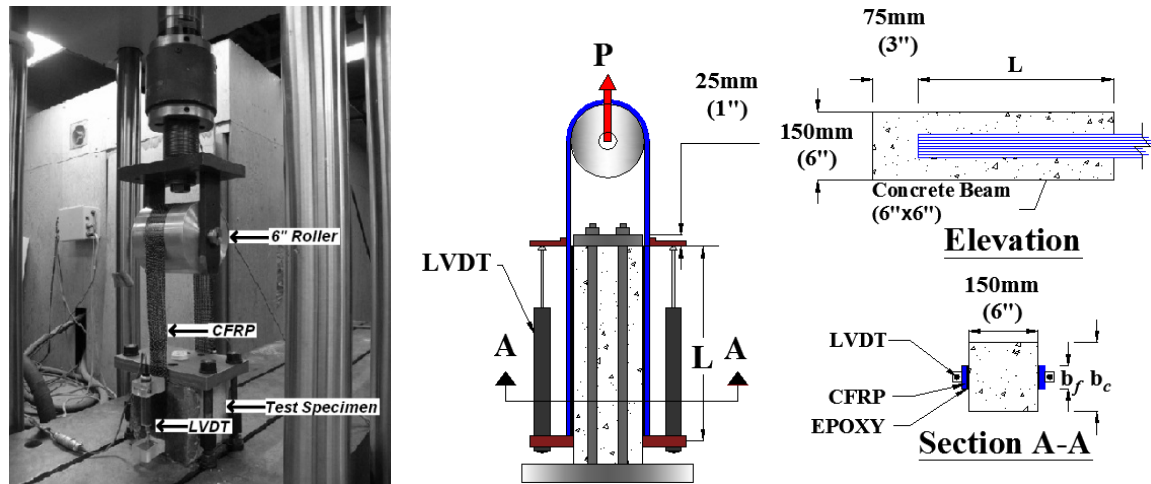


Figure 1. Typical layout of bond slip test setup and specimen

Test setup

A double face shear type pullout test was designed specifically to eliminate the acting load's eccentricity on the CFRP-concrete interface (see Fig. 1). The test setup consists of a 25.4 mm (1 in.) thick steel plate with four 19.1 mm (0.75 in.) size anchor bolts, and a 152.4mm (6 in.) diameter steel smooth cylindrical roller. The diameter of the cylindrical roller was designed to match the width of the concrete prisms and assure a pure shear/sliding state mode along the CFRP-concrete interface. The plate and anchor bolts system were used to fix the concrete prism to the machine's steel bed during testing. The CFRP strip was wrapped around the cylindrical roller, and the two ends were bonded to both sides of the concrete prism using epoxy resin. The steel roller was directly attached to the load cell using mechanical fasteners. Instron 8800 hydraulic machine (capacity 225 kN) was used to apply load on the specimens. The fixture was adjusted manually so that the face of cylindrical roller is in perfect alignment with concrete block's face. Two LVDTs were mounted at each side of the CFRP-concrete interface to measure the slip/displacement while pulling out the CFRP sheet. The load and displacement readings were collected through a portable data acquisition system (model TDS-303). Eccentricity was eliminated by averaging the readings obtained from the two LVDTs readings attached on each side of the specimen.

5. Experimental Results and Discussion

Load and displacement data were collected for each specimen. The slip (s), which is the relative displacement between concrete and the CFRP strip, was measured directly from the LVDTs. The bond stress (τ) was calculated by dividing the respective pullout load (P) by the area of the bonded CFRP strip to concrete ($A_b = L \times b_f$). The P on each strip was taken as half of the overall load applied on the specimen. Max bond strength (τ_{max}) is taken as the ultimate load (P_u) divided by A_b i.e., (P_u/A_b). The τ_{max} represents the maximum value of bond stress along the bond length and the

corresponding slip (s_o) is measured from the LVDTs.

Mode of Failure

The failure of the specimens was brittle and followed by interfacial debonding of the CFRP strips from the concrete surface by removing a thin layer of concrete. For a given boundary conditions, all the tested specimens exhibited similar failure mode (i.e., interface debonding) irrespective of the concrete f'_c and b_f . Typical failure was initiated by making a peeling off sound during the early to middle stage of loading signifying the starting point of the interfacial bond delamination. When the ultimate load was approached, the CFRP strip debonded from the concrete surface following a loud noise due to the sudden release of energy. After debonding, the specimens experienced a significant loss in resistance and the load dropped gradually. Fig. 2 shows the modes of failures of specimens with different f'_c and CFRP b_f , respectively. The interface debonding of CFRP strip from the concrete surface was expected, since the bond interface of CFRP to concrete was subjected to pure shear mode during the load application. It is noteworthy to mention that the test setup for this study was designed to prevent any failure initiating by either splitting or cracking at the leading edge of the concrete prism.

The bond stress vs. slip behaviors for all specimens are shown in Fig. 3. Investigation of Fig. 3 reveals that the bond slip behavior is formed of an ascending branch and a descending or softening branch with the bond stress (τ) approaching zero at maximum slip. The test results revealed that the initial stiffness of the CFRP concrete bonding increased with the increase in b_f . It was observed during testing that the specimens with lower concrete f'_c or larger CFRP b_f experienced more brittle failure.

Effective bond length (L_e)

Maeda et al. [13] reported the concept of effective bond length (L_e). The ultimate pullout load between CFRP and concrete interface under single/double shear type specimens does not increase after a certain bond length (L); which is known as effective bond length (L_e). They proposed an empirical formula to estimate the effective bond length (L_e)

which is a function of axial stiffness ($E_f t_f$) of FRP strips. Chen and Teng [3] proposed a new formula to calculate the L_e incorporating the effect of the ultimate compressive strength of concrete (f'_c). According to Chen and Teng [3], the effective bond length increases with increasing the FRP axial stiffness ($E_f t_f$) and decreases with increasing concrete f'_c . Nakaba et al. [14] reported that the interface debonding takes place when the bond length is short (less than 100 mm). However, debonding takes place by rupturing of FRP strips or splitting of concrete when the bond length is relatively large (greater than 300 mm). Yang et al. [16], Iso [18], Lu et al. [4], and Wu et al. [17] proposed different empirical formulas to estimate the L_e . The calculated L_e using **Table 1** varies from 55 mm (2.2 in.) to 82 mm (3.2 in.) for a single layer of CFRP strips ($t_f = 0.165$ mm) and concrete f'_c of 60.7 MPa. The study adopted the Cheng and Teng model [3] to calculate the L_e because the formula incorporated both axial stiffness and f'_c . It was found to be more consistent with the test data. In this study, the L was chosen such that $L > L_e$ for all of the specimens to make sure bond failure of CFRP-concrete interface is controlled by the delamination of CFRP strips from the concrete substrata.

Effect of Bond Width (b_f)

The effect of CFRP b_f on the maximum bond stress (τ_{max}), ultimate load (P_u), and the corresponding slip (s_o) is shown in **Fig. 4**. The test results of τ_{max} , s_o , and P_u for all specimens with variable b_f (Groups I, II, and III) are reported in **Table 3**. Inspection of **Fig. 4** reveals that the τ_{max} increased and the s_o decreased as a result of increasing the CFRP b_f/b_c ratio. The change in both τ_{max} and s_o over CFRP b_f/b_c ratio demonstrates a linear trend with a good correlation coefficient (R^2 value exceeding 0.9). The P_u also increased with increasing b_f/b_c ratio (see **Fig. 4(b)**) demonstrating a linear trend between P_u and b_f/b_c . It was revealed that a 14 mm (0.55 in.) increase in b_f increased the P_u by 4.4 kN (1.0 Kips).

The experimental results of Ueda et al. [20], Tan [7], Ren [8], and McSweeney and Lopez [10] exhibited a significant increase in the P_u as a result of increasing FRP b_f . Chen and Teng [3] stated that the FRP b_f has significant effect on the load transfer from the FRP strips to the concrete blocks. If FRP b_f is comparatively narrower than the width of the concrete block, it can result in non-uniform load transfer from the FRP strip to the concrete. This behavior leads to high stress concentration at the bond interface that is close to the point of load application, thereby reducing the P_u at bond failure. This signifies that concrete blocks with smaller CFRP b_f may have experienced higher stress concentration at locations close to the leading edge of CFRP-concrete interface.

Effect of Concrete Compressive Strength (f'_c)

The effect of concrete f'_c on the τ_{max} , s_o , for different b_f/b_c is shown in **Fig. 5 & 6** respectively. Inspection of **Fig. 5** and **Fig. 6** indicates that the increase in concrete f'_c cause an increase in the τ_{max} and s_o significantly. However, it does not have any significant effect on the ultimate load P_u (See **Fig 4 (b)**); because L_e is a function of f'_c and it decreases with increasing f'_c . The maximum bond strength τ_{max} increased as a result of increasing the concrete f'_c for any particular b_f/b_c . The effect of the concrete f'_c , varying from 42.7 to 60.7 MPa, on the P_u is presented in **Fig. 4(b)**. The **Fig. 4(b)** demonstrates that the effect of concrete f'_c was very low for specimens with CFRP b_f/b_c ratio less than 0.30 but showed significant effect on the P_u for specimens with CFRP b_f/b_c above 0.40. However, the increase in concrete f'_c increases both τ_{max} and s_o significantly and demonstrates a linear increasing trend over $\sqrt{f'_c}$. The P_u increase due to concrete f'_c was observed less significant compared to other studies (Lu et al. [4] database). These studies observed that the P_u will increase as a result of increasing f'_c . Their specimens failed by either splitting of the concrete block or by stripping out a concrete chunk at the leading edge of the FRP concrete interface however, the present study observed interface debonding between CFRP and concrete surface.

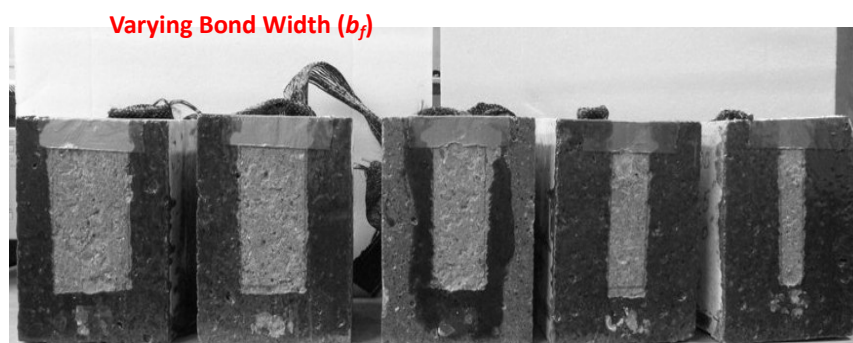
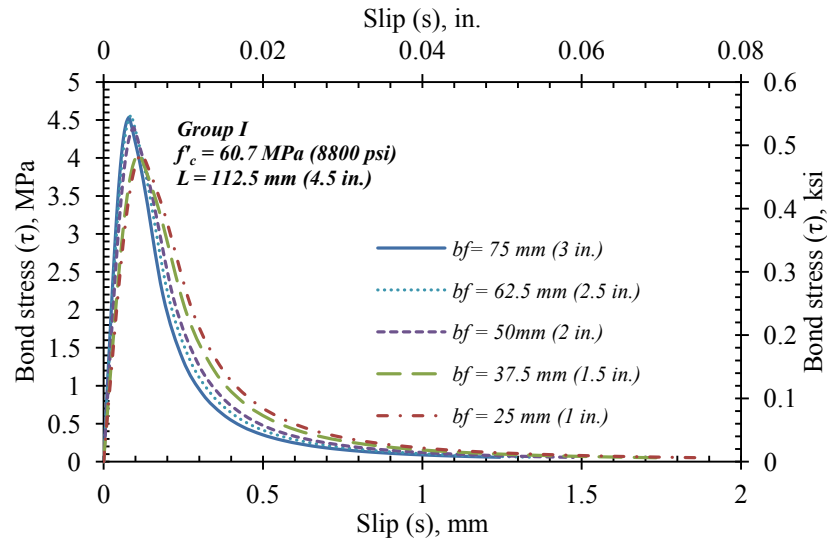
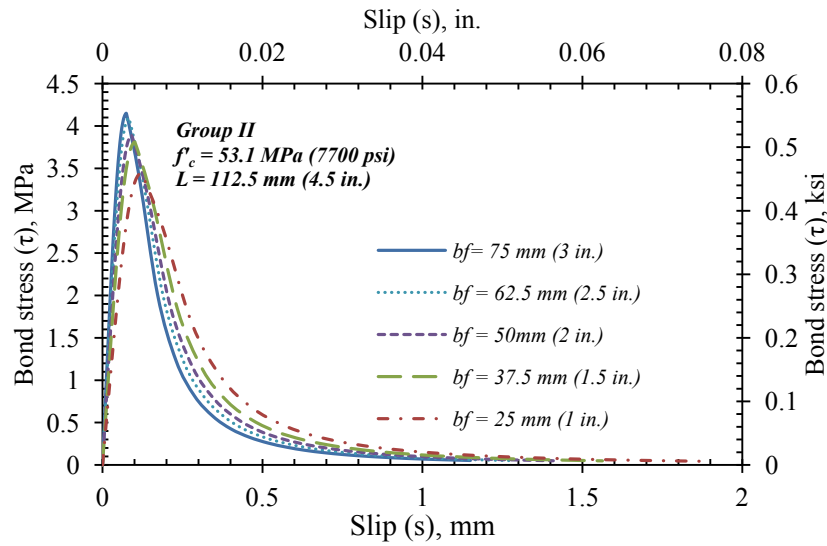
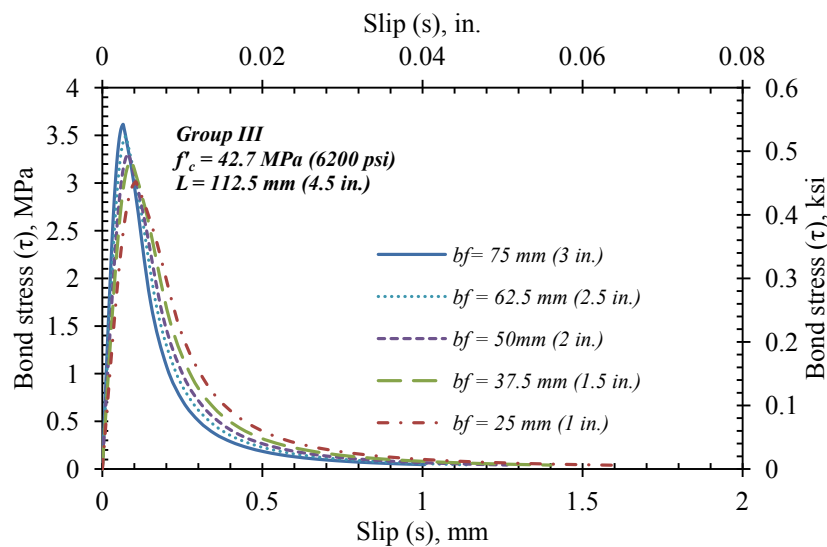


Figure 2. Mode of failure in specimens

(a) Bond stress vs. slip for Group I ($f'_c = 60.7 \text{ MPa}$; $L = 112.5 \text{ mm}$)(b) Bond stress vs. slip for Group II ($f'_c = 53.1 \text{ MPa}$; $L = 112.5 \text{ mm}$)(c) Bond stress vs. slip for Group III ($f'_c = 42.7 \text{ MPa}$; $L = 112.5 \text{ mm}$)**Figure 3.** Bond vs. Slip behavior of all the tested specimens

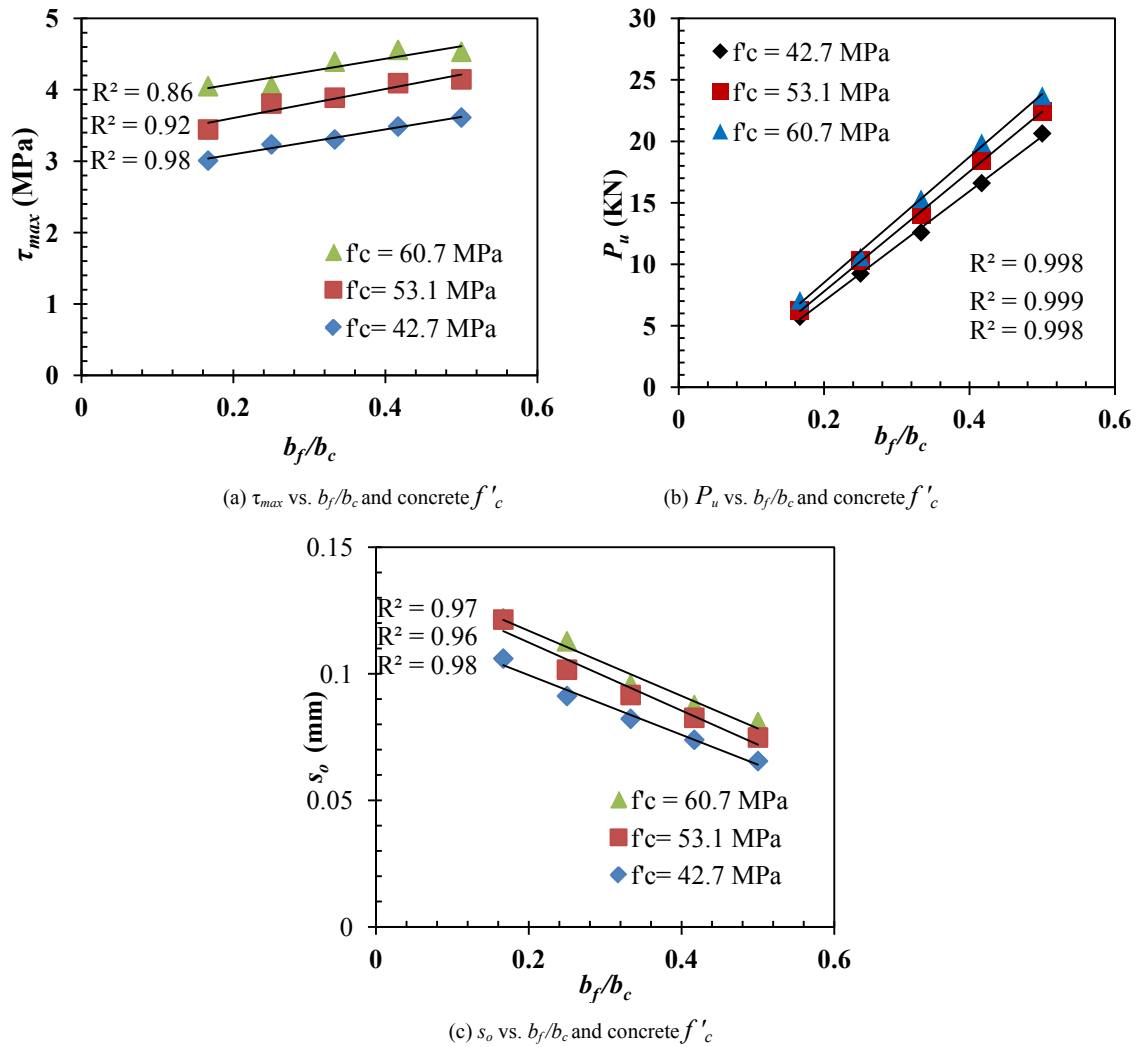


Figure 4. Effect of b_f/b_c and concrete f'_c on the maximum bond stress (τ_{max})

6. Development and Validation of Prediction Model

Development of Prediction Model for CFRP-Concrete Bond

A prediction model for P_u and s_o was proposed based on the regression analysis of the results obtained from the 30 pullout test specimens. The proposed prediction model is an enhancement of ultimate load prediction model originally proposed by Chen and Teng [3]. The model is based on prediction of effective CFRP bond area. The effective bond area is defined as $A_b = L_e \times b_f$, where L_e is the effective bond length. According to studies in literatures it was observed that τ_{max} is proportional to tensile strength of concrete which is a function of $\sqrt{f'_c}$. The data for τ_{max} for every specimen and corresponding $\sqrt{f'_c}$ of that specimen were shown in Fig 7(a). Inspection of Fig. 7(a) revealed that there is a strong linear correlation ($R^2 = 0.99$) between τ_{max} and $\sqrt{f'_c}$. Similarly, s_o and the corresponding $\sqrt{f'_c}$ for all specimen were shown in Fig. 7 (b). Fig. 7 revealed that the both τ_{max}

and s_o are affected by the change of $\sqrt{f'_c}$. The proposed equations for τ_{max} and s_o are shown in Eqs. (1) and (2):

$$\tau_{max} = \alpha_1 \beta_{w,\zeta} \beta_L \sqrt{f'_c} \quad (1)$$

$$s_o = \alpha_2 \beta_{w,s} \beta_L \sqrt{f'_c} \quad (2)$$

Where α_1 and α_2 are the regression constants; and β_w and β_L are the correction factors for CFRP b_f and L , respectively. The Equations for β_w and β_L for CFRP-concrete bond interface are given in Eq. (3)

$$\beta_{w,\zeta} = \sqrt{\left(\frac{2.25 - b_f/b_c}{1.25 - b_f/b_c}\right)} \quad (3a)$$

$$\beta_{w,s} = \sqrt{\left(\frac{2 - b_f/b_c}{1 + b_f/b_c}\right)} \quad (3b)$$

$$\beta_L = \sqrt{\left(\frac{2.25 - L/L_e}{1.25 + L/L_e}\right)} \quad (3c)$$

The α_1 values was obtained by performing regression analysis between the maximum bond stress (τ_{max}) and $\beta_{w,\zeta} \beta_L \sqrt{f'_c}$ (see Fig. 7(a)). Similarly, α_2 was found from the relation between the normalized slip at τ_{max} (s_o) and

$\beta_{w,s}\beta_L\sqrt{f'_c}$ (see **Fig. 7(b)**). Based on the regression analysis of experimental results, the values of α_1 and α_2 are 0.385, and 0.0132, respectively.

Once the τ_{max} and s_o are calculated, the ultimate load P_u can be estimated by using Eq. (4)

$$P_u = \tau_{max} b_f L \quad \text{When, } L > L_e; \quad L = L_e \quad (4)$$

The final equations for τ_{max} and s_o are listed in Eqs. 5 & 6.

$$\tau_{max} = 0.385\beta_{w,s}\beta_L\sqrt{f'_c} \quad (5)$$

$$s_o = 0.0132\beta_{w,s}\beta_L\sqrt{f'_c} \quad (6)$$

Prediction of Ultimate Load (Existing vs. Proposed Model)

According to the proposed model The experimental ultimate load can be found from Eq. (7):

$$P_u = \tau_{max} b_f L \quad \text{When, } L > L_e; \quad L = L_e \quad (7)$$

$$L_e = \sqrt{\frac{E_f t_f}{f'_c}} \quad (8)$$

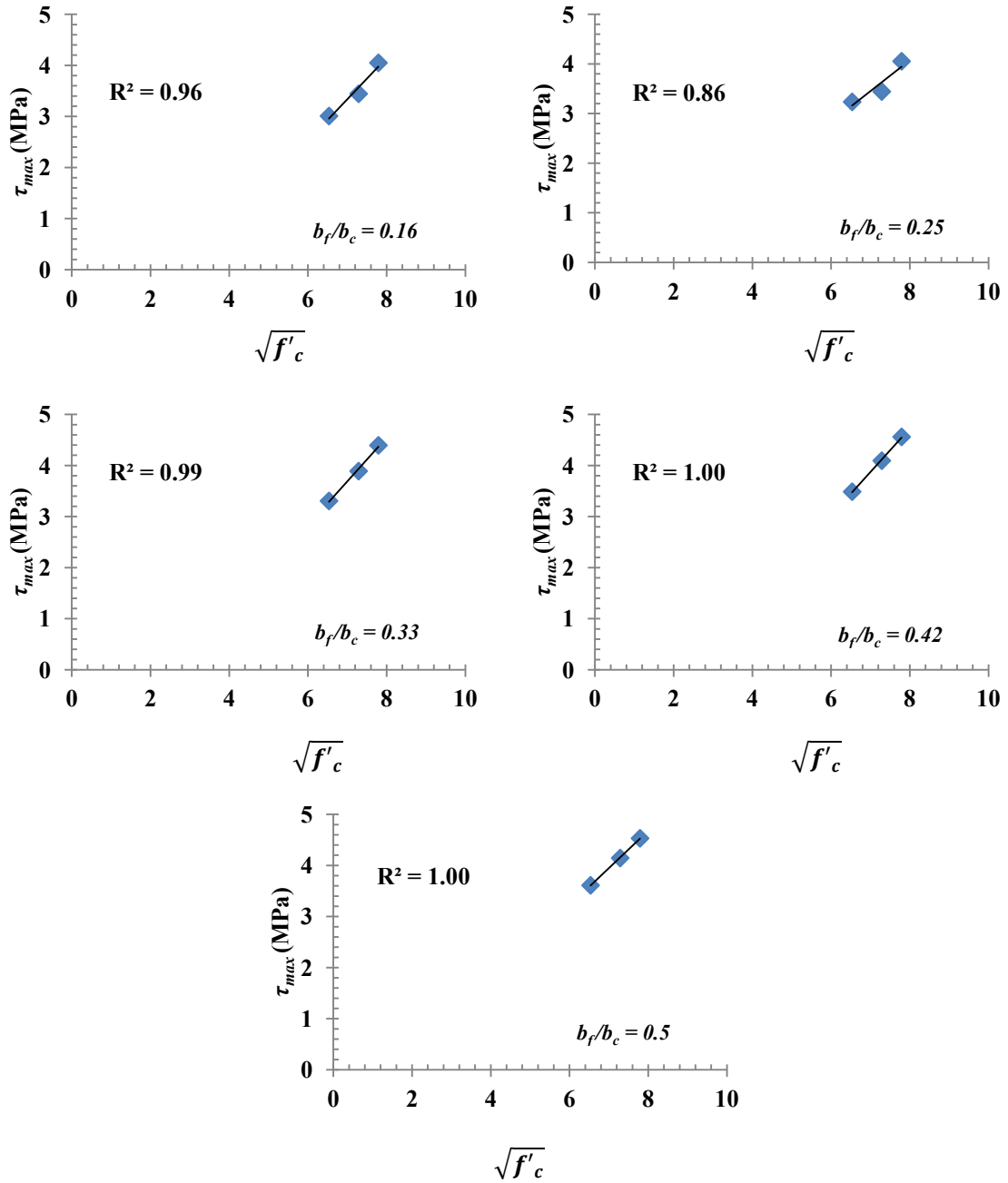


Figure 5. Effect of concrete f'_c on the maximum bond stress (τ_{max})

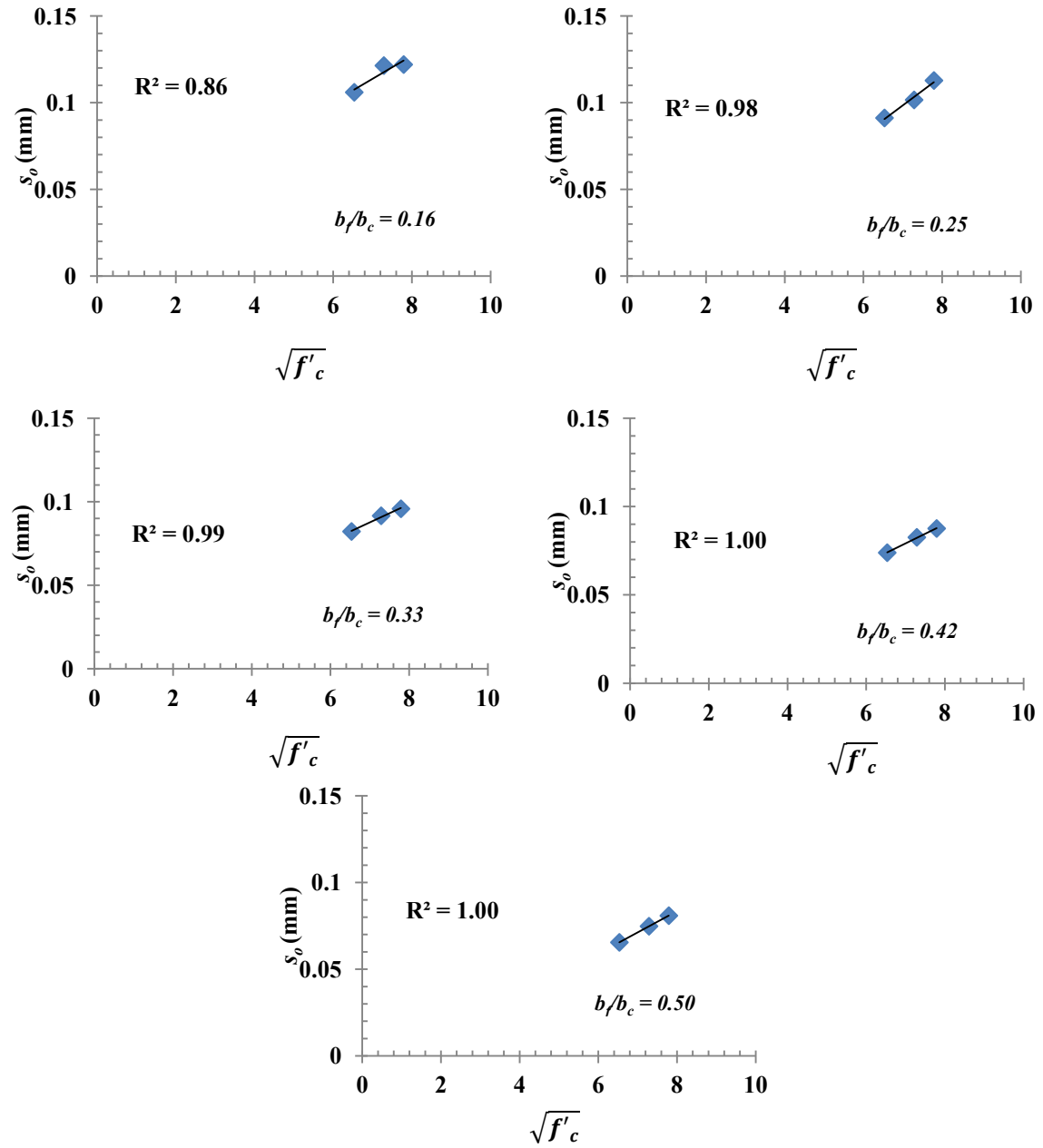


Figure 6. Effect of concrete f'_c on the slip at maximum bond stress (s_o)

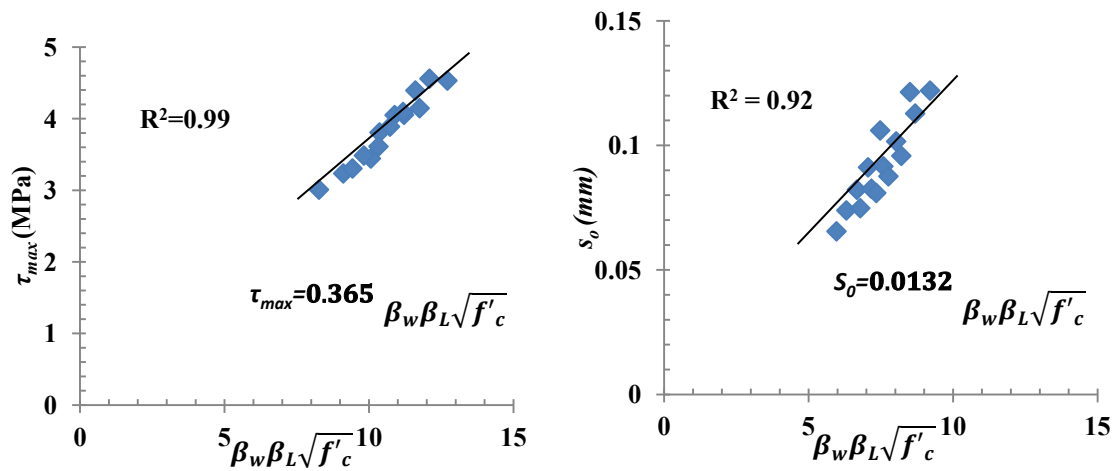


Figure 7. Relationship between maximum bond strength (τ_{max}) and slip at τ_{max} (s_o) with f'_c ratio

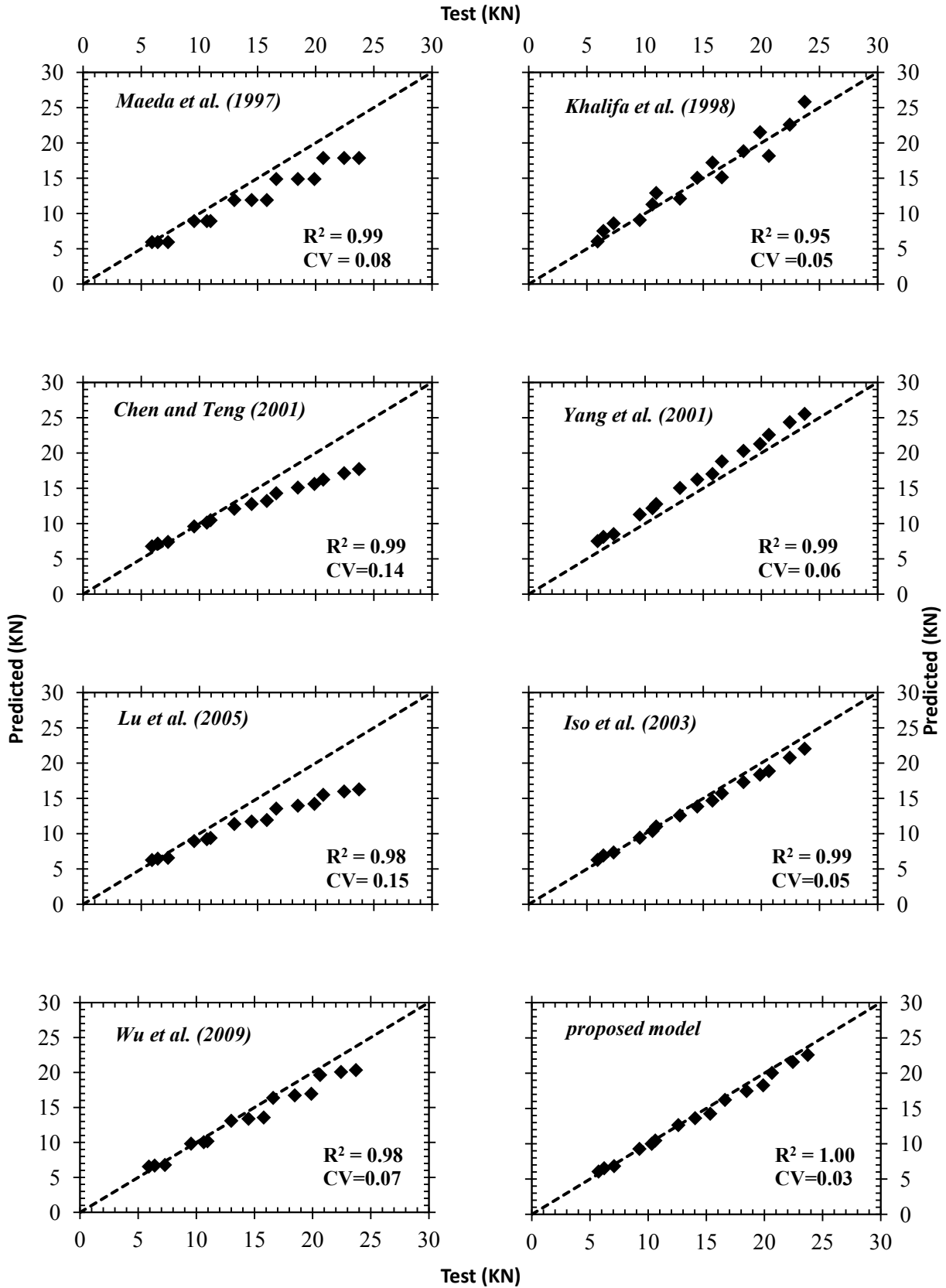


Figure 8. Proposed model and other research models for P_u vs. Experimental P_u

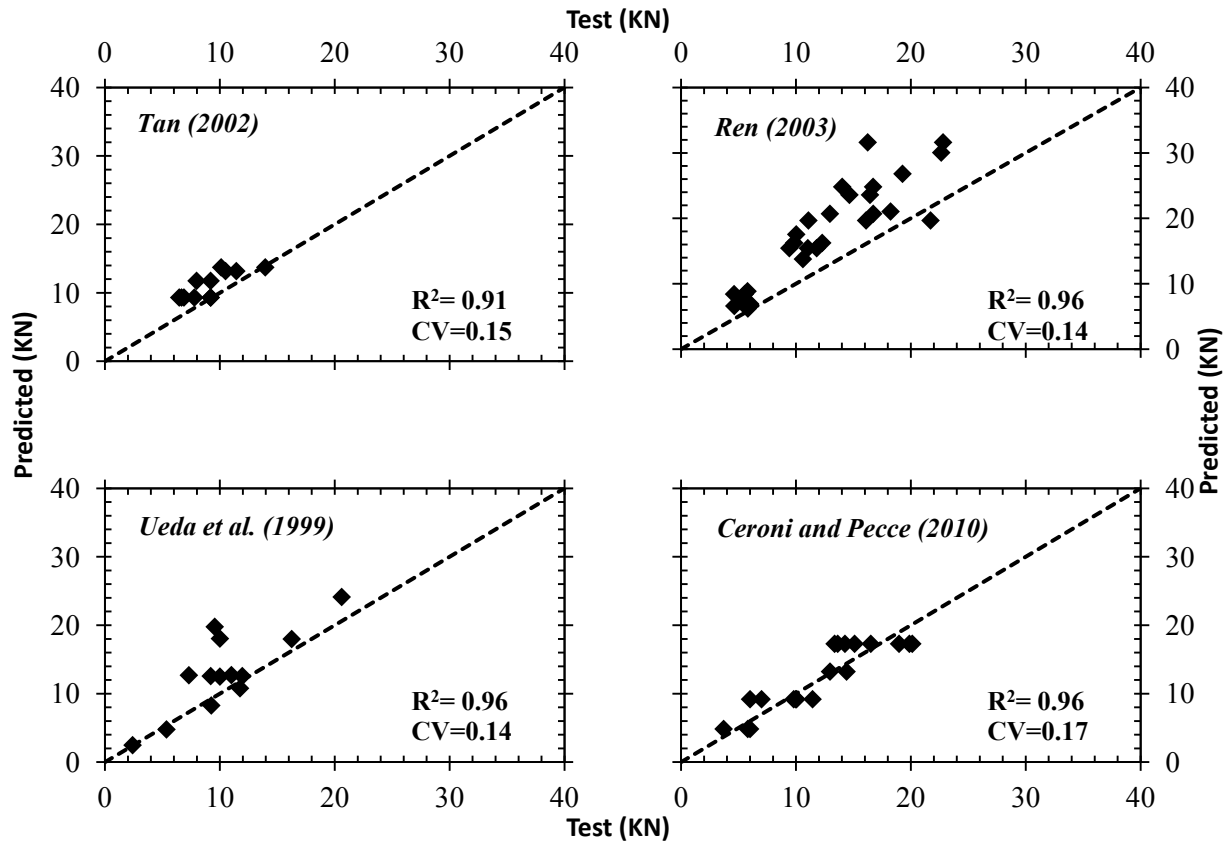


Figure 9. Validation of proposed model (P_u) with experimental P_u from other studies

Table 1 summarizes seven existing models to predict the P_u . The existing and the proposed P_u models were plotted against the experimental P_u as shown in **Fig. 8**. Inspection of **Fig. 8** reveals that the correlation coefficient (R^2) and coefficient of variation (CV) for the prediction models with respect to the experimental P_u varied from 0.96 to 1.0 and 0.05 to 0.15, respectively. This indicates that the tested results are in acceptable agreement with the existing models. The predicted results by Maeda et al. model [13] were highly scattered, because the model could not able to capture the effect of f'_c on P_u . Khalifa et al. [15] modified Maeda et al. model [13] by including the effect of f'_c on P_u . Their predicted results gave better correlation for specimens with variable b_f . Both Chen and Teng [3] and Lu et al. [4] models gave good prediction for specimens with variable b_f when their P_u was less than 15 KN; however, they underestimated the test results with P_u above 15 KN (CV=0.14 and 0.15, respectively). Wu et al. model [17] predicted results were acceptable for specimens with variable b_f when their P_u was less than 20 KN but showed some scattering (CV= 0.07) for test results with P_u above 20 KN. Yang et al. [16] and Iso et al. [18] models were observed to have the best correlation among the other existing models for specimens with variable b_f (CV=0.06 and 0.05, respectively). Their prediction models were very consistent with the experimental results. It is noteworthy to mention that all the specimens with variable b_f had a fixed L of 113 mm. Moreover, Yang et al. [16]

proposed model suggested using $L_e = 100$ mm for any FRP-concrete bond configuration with $L > 100$ mm. This assumption gave the advantage for Yang et al. model [16] to have better prediction results for specimens with variable b_f among the other existing models.

Validation of the Proposed Model

The test results of 71 specimens from existing literatures of Tan [7], Ren [8], Ueda et al. [20], and Ceroni and Pecce [21] were compared with the proposed model as shown in **Fig. 9**. The prediction of the proposed model for Tan [7] had a good correlation at the higher and lower end of P_u but showed some scattering in the middle ($R^2 = 0.91$, CV=0.15). The prediction results for Ren [8], Ueda et al. [20], and Ceroni and Pecce [21] were quite acceptable with CV of 0.14, 0.14, and 0.17, respectively. Ren [8] and Ueda et al. [20] results showed better fit for P_u values less than 14 KN. The proposed model was conservative in predicting the Ceroni and Pecce [21] P_u test results but showed overall an acceptable trend.

7. Summary and Conclusions

The experimental study was conducted to investigate the bond strength characteristics at the CFRP-concrete bond interface. The parameters considered were CFRP bond width (b_f), and the concrete compressive strengths (f'_c). A specially

designed experimental testing setup using a double face shear type pullout test was implemented. The testing setup was capable of eliminating the eccentricity of active load, and ensure a pure shear failure across the CFRP-concrete bond interface. An analytical model was developed based on Chen and Teng [3] model to assess the maximum bond strength (τ_{max}), slip at max stress (s_o). The following conclusions can be drawn:

1. The test results revealed that for a given boundary conditions all the tested specimens exhibited similar failure mode (i.e., interface debonding) irrespective of the concrete f'_c and CFRP b_f . The failure of the specimens was brittle and followed by interfacial debonding of the CFRP strips from the concrete surface by removing a thin layer of concrete.

2. CFRP b_f has significant effect P_u . The increase in CFRP b_f increases the P_u . The CFRP strips with wider b_f increased the τ_{max} and reduced the s_o . The τ_{max} increase was observed to be influenced by the b_f/b_c ratio.

3. The higher the concrete f'_c the higher the τ_{max} and s_o . However, the concrete f'_c effect was less pronounced on P_u .

4. The experimental P_u was observed to have good fit with the existing models for specimens with variable CFRP b_f and f'_c .

5. The proposed model was compared with other models using experimental results from the literature. It was found that the proposed model is equally capable like other existing models in predicting the P_u .

Notation

The following symbols are used in this paper.

A_b = Area of bonded CFRP strip, mm² (in²)

b_f = bond width of CFRP strip, mm (in.)

E_f = Modulus of elasticity of CFRP strip, MPa (psi)

f'_c = 28 days concrete compressive strength, MPa (psi)

f_t = Tensile strength of concrete per ACI 318-11 ($7.5 \sqrt{f'_c}$), MPa (psi)

G_f = Interfacial fracture energy at the CFRP-concrete interface, N.mm/mm² (lb.in/in²)

L = bond length of CFRP strip, mm (in.)

L_e = effective bond length of CFRP strip, mm (in.)

P_u = Ultimate load capacity of the bond between CFRP and concrete, KN (Kip)

s = bond slip at the CFRP-concrete interface, mm (in.)

s_o = bond slip at the mean bond strength (τ_{mean}), mm (in.)

t_f = CFRP strip, mm (in.)

τ = Bond stress at the CFRP-concrete interface = $P/(b_f \times L)$, MPa (psi)

τ_{max} = Maximum bond strength at the CFRP concrete interface = $P/(b_f \times L_e)$, MPa (psi)

β_w = CFRP to concrete width ratio factor

β_L = CFRP to concrete effective length to actual length ratio factor

REFERENCES

- [1] ACI Committee 440.2R. "Guide for the Design and Construction of Externally Bonded FRP Systems for Strengthening Concrete Structures," *American Concrete Institute*, (2008), Farmington Hills, Michigan.
- [2] Canadian Standards Association (CSA). "Design and construction of building structures with fibre-reinforced polymers." *CSA806-12*, (2012), Mississauga, ON, Canada.
- [3] Chen, J.F. and Teng, J.G. "Anchorage strength models for FRP and steel plates bonded to concrete", *Journal of Structural Engineering ASCE*, (2001), V. 127, No.7, pp.784-791.
- [4] Lu, X. Z., Teng, J.G., Ye, L.P., and Jiang, J. J. "Bond-slip models for FRP sheets/plates bonded to concrete", *Engineering Structures, Elsevier*, (2005), V.27, No.6, pp. 920-937.
- [5] Takeo, K., Matsushita, H., Makizumi, T., and Nagashima, G. "Bond Characteristics of CFRP Sheets in the CFRP Bonding Technique", *Proc. Japan concrete institute*, (1997), Vol. 19, No. 2, pp. 1599-1604.
- [6] Wu, Z., Yuan, H., Yoshizawa, H., and Kanakubo, T. "Experimental/analytical study on interfacial fracture energy and fracture propagation along FRP-concrete interface", *ACI International*, (2001), SP-201-8, pp. 133-152.
- [7] Tan, Z. "Experimental Research for RC Beam Strengthened with GFRP", M.S. Thesis, (2002), Tsinghua University, China. [in Chinese].
- [8] Ren, H. T. "Study on Basic Theories and Long Time Behavior of Concrete Structures Strengthened by Fiber Reinforced Polymers", Ph.D Thesis, (2003), Dalian University of Technology, China. [in Chinese].
- [9] Dai, J., Ueda, T., and Sato Y. "Development of the Nonlinear Bond Stress-Slip Model of Fiber Reinforced Plastics Sheet-Concrete Interfaces with a Simple Method." *J. Compos. Constr.*, (2005), V. 9, No 1, pp. 52-62.
- [10] McSweeney, B.M., and Lopez, M.M. "FRP-Concrete Bond Behavior: A Parametric Study Through Pull-Off Testing", *ACI International*, (2005), SP-230-26, V. 230, pp. 441-460.
- [11] Fawzia, S., Zhao, X.L., and Al-Mahaidi, R. "Bond-slip models for double strap joints strengthened by CFRP", *Composite Structures, Elsevier*, (2010), V. 92, No. 9, pp. 2137-2145.
- [12] Ko, H., Matthys, S., Palmieri, A., Sato, Y. "Development of a simplified bond stress-slip model for bonded FRP-concrete interfaces", *Construction and Building Materials*, (2014), Volume V. 68, No. 15, Pages 142-157.
- [13] Maeda, T., Asano, Y., Sato, Y., Ueda, T., and Kakuta, Y. "A study on bond mechanism of carbon fiber sheet". *Proc. 3rd international symposium on non-metallic (FRP) reinforcement for concrete structures*, (1997), Japan Concrete Institute, Sapporo, vol. 1. p p. 279-85.
- [14] Nakaba, K., Kanakubo, T., Furuta, T., and Yoshizawa, H. "Bond behavior between fiber reinforced polymer laminates and concrete", *ACI Structural Journal*, (2001), V.98, No.3, pp. 359-67.

- [15] Khalifa, A, Gold, W.J., Nanni, A., and Aziz, A. "Contribution of externally bonded FRP to shear capacity of RC flexural members". *Journal of Composites for Construction, ASCE*, (1998), V. 2, No. 4, pp. 195–203.
- [16] Yang, Y.X., Yue, Q.R., and Hu, Y.C. "Experimental study on bond performance between carbon fiber sheets and concrete", "Journal of Building Structures" (2001), V. 22, No. 3, pp. 36–42. [in Chinese]
- [17] Wu, Z., Islam, S.M., and Said, H. "A Three-Parameter Bond Strength Model for FRP–Concrete Interface", *Journal of Reinforced Plastics and Composite*, (2009), V. 28, No. 19, pp. 2309–2323.
- [18] Ahmed, E.Y. S., Bakay, R., and Shrive, N.G. "Bond Strength of FRP Laminates to Concrete: State-of-the-Art Review", *Electronic Journal of Structural Engineering*, (2009), Vol. 9, pp. 45–61.
- [19] Ferrier, E., Quiertant, M., Benzarti, K., and Hamelin, P. "Influence of the properties of externally bonded CFRP on the shear behavior of concrete/composite adhesive joints", *Composite Part B: Engineering, Elsevier*, (2010), V.41, No. 5, pp. 354–362.
- [20] Ueda, T., Sato, Y., and Asano, Y. "Experimental Study on Bond Strength of Continuous Carbon Fiber Sheet", *ACI International*, SP-188-37, (1999), V. 188, pp. 407–416.
- [21] Ceroni, F., and Pecce, M. "Evaluation of Bond Strength in Concrete Elements Externally Reinforced with CFRP Sheets and Anchoring Devices." *J. Compos. Constr.*, (2010) V. 14, No. 5, pp. 521–530.